Optimal Synthesis of a High Purity Bioethanol Distillation Column Using Ionic Liquids

ARTICLE *in* INDUSTRIAL & ENGINEERING CHEMISTRY RESEARCH · DECEMBER 2010

Impact Factor: 2.59 · DOI: 10.1021/ie101801c

3 AUTHORS, INCLUDING:

Ruben Vasquez-Medrano
Universidad Iberoamericana Ciudad de México
29 PUBLICATIONS **276** CITATIONS
SEE PROFILE

Antonio Flores
Tecnológico de Monterrey
80 PUBLICATIONS **791** CITATIONS
SEE PROFILE

I&EC research
Industrial & Engineering Chemistry Research

ARTICLE

pubs.acs.org/IECR

Optimal Synthesis of a High Purity Bioethanol Distillation Column Using Ionic Liquids

Luz Maria Chávez-Islas, Ruben Vásquez-Medrano, and Antonio Flores-Tlacuahuac*

Departamento de Ingeniería y Ciencias Químicas, Universidad Iberoamericana Prolongación Paseo de la Reforma 880, México D.F., 01210, México

ABSTRACT: In this work, we address the optimal economical synthesis of an extractive distillation column for bioethanol purification, using ionic liquids as a type of solvent that can be designed to feature sustainable characteristics, such as low toxicity and low volatility, among other desirable properties. For the optimal synthesis of the separation scheme, we propose a mixed-integer nonlinear programming (MINLP) formulation, merged with disjunctive programming tools, to take care of modeling logical decisions [Yeomans and Grossmann, *Ind. Eng. Chem. Res.* **2000**, *39*, 1637−1648]. In a previous work [Chavez-Islas et al., submitted to *Ind. Eng. Chem. Res.*], we have addressed the design of a novel ionic liquid to separate the ethanol/water azeotropic system, up to high purities. The MINLP synthesis of the distillation column considers the feed tray location, the number of trays, and the operating and design parameters as decision variables. Because the ionic liquid used in this work is a novel solvent, its physical and thermodynamic properties are yet not available. Therefore, the physical properties of the ionic liquid are estimated using group contribution methods. The MINLP formulation is based on the application of the MESH equations for conditional trays, to reduce the size of the nonlinear subproblems and increase the robustness of the optimization formulation. The MINLP problem was solved using the SBB solver embedded in GAMS. Using the proposed MINLP formulation, we attained ethanol purities as good as 99.9 mol %, and 90% of the ethanol presented in the feed stream was recovered.

1. INTRODUCTION

The supply of energy for various operations such as transportation, power generation, and heating is of critical concern in the world today. In fact, in the U.S. economy, approximately one-third of all energy consumption can be attributed to the transportation sector,[3] and probably similar figures exist in other world economies. Fossil fuels such as coal and crude oil, which have been the traditional source of energy, are nonrenewable and have been identified as one of the main emission sources of carbon dioxide and sulfur oxides. Moreover, fossil fuel reserves are being increasingly depleted and prices of fossil fuels have significantly increased recently. Carbon dioxide has been related to the greenhouse effect, which is responsible for global warming, whereas sulfur dioxide is responsible for acid rain effects. These reasons, along with increasing concerns about global warming and public health issues, have led to a search for new sustainable energy alternatives to fossil fuels. Hence, the use and development of sources of alternative energies, such as solar, wind, and geothermal energies, as well as fuel cells, batteries, and biofuels, have become a priority.

In this work, we are mainly concerned with the manufacturing of a type of renewable fuel using biomass feedstock. Renewable fuels obtained from biomass are commonly known as biofuels, and they include ethanol, butanol, biodiesel, and hydrogen. It has been stated that, by 2022, one-third of the U.S. petroleum energy requirements should be replaced by fuels produced from biomass.[4] At least half of that requirement will be covered by ethanol production (∼16 billion gal/yr).[3] Therefore, new, optimal, and renewable ways of approaching the purification of alcohol/water azeotropic mixtures are required and justified. On the other hand, biomass can also be used for the production of other chemical compounds, such as furfural, which is used in the synthesis of nylon 6,6. On a minor scale, biomass may also be used for power generation. Chemical plants producing biofuels, chemical compounds, and power generation have become known as biorefineries.[5] In the near future, some petrochemical industry tasks will be carried out in biorefineries. This is particularly true regarding fuels and chemical products manufacturing. Biomass is a widely available feedstock and includes corn, sugar cane, cellulosic residues, algae, etc. Because corn and sugar cane are food crops, it may be more reasonable to use cellulosic residues and algae as raw materials for biorefineries. On the other hand, presently, the cost of biofuels (i.e., bioethanol) is larger, in comparison to the cost of energy from fossil fuels. This is a serious handicap for the use of alternative energy sources. However, there are some ways to reduce this gap, and one of them refers to the use of optimization tools in energy systems. From a Process Systems Engineering point of view, the cost of bioethanol can be reduced, addressing the purification step that turns out to be the most expensive operation in ethanol manufacturing. Hence, one of our objectives in the present work lies in the economical optimal synthesis of the purification operation, using a novel type of sustainable solvent known as an ionic liquid.[6,7]

Special Issue: Puigjaner Issue

Received: August 27, 2010
Accepted: November 8, 2010
Revised: November 6, 2010
Published: December 31, 2010

As mentioned above, one of the major hurdles in switching to a biomass-based industry is the production costs (both economic and energetic) of the alcohols. Purifying an alcohol requires ~6% of the energetic value of the compound itself, with a large portion used in the separation of the alcohol from the fermentation broth, which is mainly composed of water.[8] The average energy requirement per liter of ethanol produced is 2446 kcal.[9] In the separation of the ethanol/water system, the formation of azeotropes does not allow the separation by simple distillation. Conventionally, separating alcohols and water requires a series of distillation columns. This method is energetically costly, and much room for improvement exists. Recent development of new membrane technology, such as pervaporation, has improved the efficiency of this separation, although rapid fouling of the membranes remains a major issue with these methods.[10] Drying over zeolites has also been widely used to address the above-mentioned separation task.

Other separation schemes that have been used to carry out the ethanol/water separation requires a conventional distillation column, coupled with a set of membrane modules,[11,12] pressure-swing distillation columns,[13,14] wall-divided distillation columns,[15,16] and extractive distillation, and there are some other more-conventional separation schemes that use heat-integrated distillation columns and posterior processing using membranes.[17] Extractive distillation is a separation process used to separate mixtures that are difficult or impossible to separate by conventional distillation; a third component (solvent or entrainer) is added to the binary mixture to increase the relative volatility of the original components.[18] For ethanol−water separation using extractive distillation, a solvent such as ethylene glycol or benzene is used. Solvents comprise two-thirds of all industrial emissions and one-third of all volatile organic content (VOC) emissions nationwide. These emissions have been linked to a host of negative effects, including global climate change, poor urban air quality, and human illness.

The new constraints facing chemical engineers involve continuing to provide society with the products necessary to sustain a high standard of living, while, at the same time, significantly reducing the environmental impact of the industrial processes used for this objective. Achieving these apparently contradictory objectives is one of the great challenges facing science and technology in the coming decades. Along these lines, some of the present hazardous chemical compounds used in industry must be replaced by new sustainable, nontoxic, nonvolatile, and biodegradable compounds. In a previous publication, we have addressed the design of a new type of sustainable solvents for high-purity ethanol purification.[2] This is an example of how product design can provide some of the new required sustainable materials.

Recently, there has been a growing interest in the use of new types of solvents, known as ionic liquids (ILs),[19] that may become a key ally in helping society to meet the challenges of efficient and environmentally benign chemical processing. They have the potential to revolutionize the way we think of and use solvents. In particular, they have been proposed for the separation of alcohol/water azeotropic systems,[20] using simple extractive distillation or liquid−liquid extraction and, generally, for the separation of azeotropic mixtures.[21] Some initial process design for ethanol[22] and butanol[23] purification also has been advanced. ILs are a combination of asymmetric and bulky organic cations with organic or inorganic anions. This factor tends to reduce the lattice energy of the crystalline structure of the salt and, hence, lower their melting point so that they generally remain liquid at or near room temperature. Unlike molecular liquids, the ionic nature of these liquids results in an unique combination of properties, namely, high thermal stability, large liquids range, negligible vapor pressure, inflammability, and the ability to dissolve many different organic, inorganic, and organometallic compounds, determining their high potential as green solvents.[7,24] Furthermore, ILs present the prospective of "designer solvents", since their physicochemical properties can be finely tuned by a criteria's choice of the cation and the anion. As a result, these solvents can be designed for a particular application or to present a particular set of intrinsic properties. ILs feature several interesting properties. Perhaps the most intriguing feature of these compounds is that, although they are liquid in their pure state at room temperature, they have essentially no vapor pressure. They do not evaporate; therefore, they cannot lead to fugitive emissions. Many of these compounds are liquids over large temperature ranges, from below ambient to well over 300−400 °C, which suggests that they could be used under unique processing conditions.[6] Moreover, They act as entrainers for a great variety of azeotropic systems. Especially if water is one component of the azeotrope very high separation factors can be achieved. ILs usually are quite hygroscopic materials, which shows their strong affinity to water. The IL literally captures the water and releases the second compound, which can be distilled off as pure material. In other words, the IL is acting as an extracting agent for water and the process is then called extractive distillation. The advantage of an IL over a classic entrainer is that ILs have extremely low vapor pressure and can be neglected. This means that the entrainer itself does not need to be distilled and, hence, a second distillation column is not necessary and a significant amount of energy can be saved.[25] Although ILs can be used for difficult separation tasks and possess some desirable properties (i.e., low toxicity levels), they can have some hidden negative environmental impacts related to their manufacture and raw materials used to synthesize them. To get a better idea about their environmental impact, a life cycle assessment should be performed.

In this work, we are mainly concerned about the optimal economic synthesis of an extractive distillation column used for the purification of the ethanol/water azeotropic system up to the high purities normally required for using ethanol in the transportation sector. One of the novelties of the present work lies in the use of a new type of sustainable solvent—ILs—that possess some challenges, mainly because we have to be sure that the IL actually leads to the separation of the addressed azeotropic system. In a previous work,[2] we addressed the optimal molecular design of an IL for the ethanol/water separation of an E85 system (a mixture that contains 85 mol % ethanol and 15 mol % water). The resulting IL is 1-ethyl-3-methylimidazolium dimethylphosphate (denotes hereafter as [emim][DMP]). This IL guarantees an ethanol purity of ≥99 mol % and an ethanol flow recovery of 90%. The distillation column synthesis is based on the superstructure for a simple column developed by Yeomans and Grossmann,[1] with some modifications being attributable to the presence of ILs. A similar approach for the design of ILs using an optimization approach has been recently proposed.[26]

The outline of this paper is as follows. In the next sections, we describe the problem and the methodology, where a superstructure and the premises considered to solve the problem are described, a detailed formulation of the MINLP model applying the generalized disjunctive programming, results and analysis of

results, and conclusions of the work. In the results section, the optimal configuration of the extractive distillation column, minimizing an economical function with the products fulfilling minimal specifications of purity and recovery, is presented.

2. PROBLEM FORMULATION

The problem to be solved can be stated as follows. Given is a set of two feed streams, composed of an ethanol/water mixture and a priori designed IL suitable for the intended separation, whose flow rate, composition, temperature, and pressure are known and a set of distillation and bottoms products with target purities and recoveries. Also given is a specified maximum number of separation trays in the column; constant pressure along the column is also assumed. The problem then consists of determining the optimal number of trays and the ethanol/water feed tray location, as well as the design and operating parameters, such as reflux ratio, column diameter, vapor and liquid internal flow rates, tray temperatures, composition of the internal vapor and liquid streams, condenser and reboiler areas, and their heat duties, such that the total annualized cost (TAC) of equipment and utilities is minimized. The design of the IL, which is suitable for the addressed separation, using an optimization approach, has been undertaken elsewhere.[2]

3. OPTIMIZATION FORMULATION

The methodology used for the optimal process design first consists of the development of the alternative superstructures for the optimal economical design of the extractive distillation column, such that it guarantees that the products meet the target specifications. The second step is concerned with the formulation of the objective function and the set of constraints to be met. Commonly, the objective function and associated constraints feature the set of modeling assumptions stated for formulating the optimization model. The two steps of the above-mentioned process design methodology will be detailed next.

Extractive Distillation Column Superstructure. The basic element to model a distillation column is the equilibrium stage, which is represented by a separation tray in the column. In the present work, the minimum number of stages of the extractive distillation column turns out to be four: the feed stage of the ethanol/water azeotropic mixture, the feed stage of the IL, the condenser stage, and the reboiler stage. Those stages are always present in the column. Therefore, they are considered permanent elements of the optimization model. On the other hand, there are some other trays located in the stripping and rectifying sections, whose presence is dependent on factors such as target purity, separation cost, and operating process conditions. We will refer to those trays as conditional trays, and they also will be treated as decision variables.

The superstructure proposed in this work explicitly identifies the tasks that take place in the permanent and conditional trays. Figure 1 shows the superstructure of the extractive distillation column, setting the difference between the permanent and conditional trays. The permanent tray of the IL feed stream is located immediately below the condenser tray. For each permanent tray in the column, the mass transfer tasks are taken into account and modeled using the MESH equations, namely, the component mass balances, the tray energy balance, the physical equilibrium equations, and the summation of liquid and vapor mole fractions. As aforementioned, the conditional trays can or cannot be part of the final optimally synthesized column.

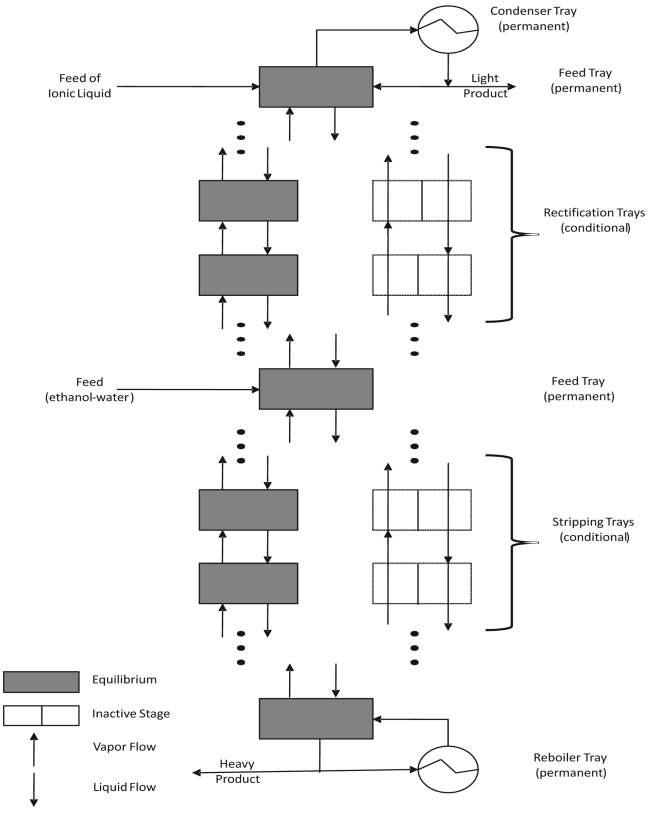

Figure 1. Schematic of the extractive distillation column superstructure.

Normally, upper bounds for the number of conditional trays in the stripping and rectifying zones of the columns are specified and part of the optimization problem lies in the determination of the optimal number of trays in each separation section. As a result of this decision, the optimal location of the feed tray is also obtained. In summary, for the modeling of a conditional tray, the MESH equations are directly applied. However, for a nonexisting or inactive tray, the MESH equations are simply replaced by an input−output operation with no mass transfer, which gives rise to trivial mass and energy balance equations (inlet and outlet flows and enthalpy are the same for the liquid flows and vapor flows).

Note that previous work on the optimization of distillation separation[27] required one to include the MESH equations, even for nonexisting trays. The result was that such mixed-integral nonlinear programming (MINLP) problems were rather hard to solve. The use of logic in mathematical programming[28,29] allows one to model only those elements that are really part of the final optimization formulation, increasing the numerical robustness of optimization problems in general and of MINLP problems in particular. Generalized Disjunctive Programming (GDP)[1,30−32] has been widely used to model logic decisions in mathematical programming. There are some other approaches, such as complementarity constraints,[33−35] that could be used for the same purpose. An important difference between the GDP approach and complementarity constraints for handling logic-based optimization problems is that GDP requires the introduction of binary variables, whereas complementary constraints do not need the introduction of such variables. However, from our point of view, presently, optimization formulations based on GDP seems to be easier to handle. Moreover, there are few available

algorithms for the efficient solution of equilibrium constraint problems.[36] To optimize the steady-state design of a distillation column, Yeomans and Grossmann[1] proposed a GDP model, which is solved with a modification of the logic-based outer approximation (OA) algorithm of Turkay and Grossmann.[37] This decomposition algorithm solves the problem by iterating between reduced NLP subproblems and a MILP master problem. The NLP subproblem contains only the equations for the terms in the disjunctions that are true and provides an upper bound of the objective function value. The master problem predicts a combination of discrete variables, which is optimal for the global linear approximation of the problem.

In this work, we will approach the optimization modeling of logic decisions using the GDP approach and the big-*M* framework for MINLP reformulation. Moreover, we extend the MINLP formulation proposed in ref 1 for handling separations that use ILs to achieve high purity and recover ethanol/water azeotropic mixtures. For this purpose, we consider the use of a previously optimally synthesized IL[2] that is capable of carrying out the intended ethanol/water azeotropic separation task, up to high ethanol purity. The reader is referred to ref 2 for details about the optimal molecular design of the IL. Because the IL was designed to feature negligible vapor pressure, we will assume that it is only present in the liquid phase. The IL is treated as a nondissociated component and the vapor-phase thermodynamic behavior is assumed to be ideal, because the extractive column will be operated at constant atmospheric pressure. Hence, the vapor-phase fugacity coefficients are unity. However, the effect of the IL is taken into account when the liquid-phase activity coefficients are calculated. The activity coefficients are determined using the extension to ionic liquids of the UNIFAC method. Notice that, because the IL is not present in the vapor phase, some modifications to the MESH equations are required to handle this fact. The MESH equations in our system do not include the phase equilibrium equation of the IL because this component is not present in the vapor phase. Instead of this equation, in this work total mass balances around the envelope in the rectifying and in the stripping sections of the column, without considering the ethanol/water feed tray, are proposed. With this modification, the IL material balances are met in each stage of the distillation column. From Figure 2, it can be observed that the envelopes above the ethanol/water feed tray include the condenser tray, the IL feed tray, and active trays in the rectifying zone. In a similar way, the stripping section envelops around the reboiler and the active trays are considered. This type of balance is applied for each active tray defined in the optimal configuration of the column, except the condenser, the reboiler, and the ethanol/water mixture feed trays. The condenser is a total condenser.

MINLP Problem Formulation. In this section, we present the detailed MINLP GDP model for the optimal economical design of the extractive distillation column. The meaning of all variables is contained in the Nomenclature section.

Objective Function. The optimization of the distillation column is carried out by minimizing a combination of both investment costs and operating costs. The objective function reads as follows:

$$\begin{aligned}\min_{u}\ \mathrm{TAC} &= \mathrm{ICC}\cdot f(\mathrm{NT},\mathrm{CD}) + \mathrm{IACRA}\cdot f(\mathrm{RA}) \\ &\quad + \mathrm{IACCA}\cdot f(\mathrm{CA}) + \mathrm{SUC}\cdot f(\mathrm{QR}) \\ &\quad + \mathrm{CUC}\cdot f(\mathrm{QC}) - \mathrm{CP}_{\mathrm{C_2H_5OH}}\cdot f(D_{\mathrm{C_2H_5OH}}) \end{aligned} \tag{1}$$

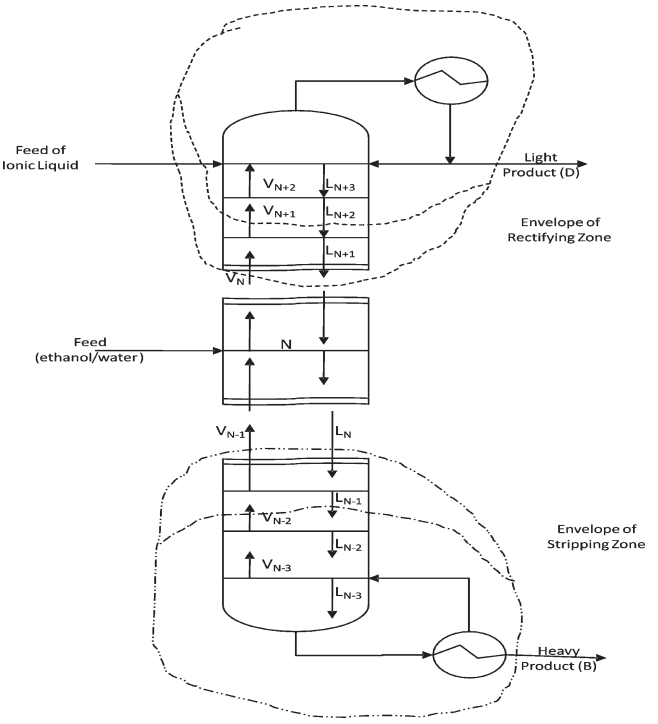

Figure 2. Schematic describing the rectifying and stripping zone envelopes.

where **u** represents the set of decision variables. ICC, IACRA, IACCA, SUC, CUC, and $\mathrm{CP}_{\mathrm{C_2H_5OH}}$ are coefficients of the cost functions whose values are 0.162844, 0.1782, 0.1782, 4.173×10^{-3}, 7.48×10^{-4}, and 1.25×10^{-4}, respectively. The cost functions are defined as follows:

$$f(\mathrm{NT},\mathrm{CD}) = (\mathrm{NT})(\mathrm{CD}^{1.245}) \tag{2}$$

$$f(\mathrm{RA}) = \mathrm{RA}^{0.8} \tag{3}$$

$$f(\mathrm{CA}) = \mathrm{CA}^{0.8} \tag{4}$$

$$f(\mathrm{QR}) = 8000\mathrm{QR} \tag{5}$$

$$f(\mathrm{QC}) = 8000\mathrm{QC} \tag{6}$$

$$f(D_{\mathrm{C_2H_5OH}}) = 8000\mathrm{C_2H_5OH} \tag{7}$$

Optimization Model Constraints. The set of constraints for the optimization formulation can be classified in two wide groups. The first group includes constraints featuring only continuous variables, because they refer to permanent trays, such as feed trays, condenser trays, and reboiler trays. The second group includes constraints involving discrete decisions that contain both continuous and boolean variables (disjunctive constrains). The constrains related to the second group are valid for specific column configurations, depending on if vapor−liquid equilibrium (VLE) equations are applied to a given tray.

Continuous Constraints. The continuous constraints include the general column mass balance, the purity and recovery requirements, the calculation of the number of stages, column diameter, reboiler and condenser areas. These constraints are given as follows

(to save notation, when the elements of the set i are not specified, it is understood that such elements are ethanol and water):

• General column component mass balance

This constraint takes into account all of the streams that are fed into the column and the bottom and top products to set up the component mass balance.

$$\sum_{n \in \mathrm{NFT}} F_n^i = D^i + B^i \qquad i \in C \tag{8}$$

• Recovery of component i in the distillate and bottoms product.

$$D^i \geq \xi_c^i \cdot F^i \qquad i = \{\mathrm{C_2H_5OH}\} \tag{9}$$

$$B^i \geq \xi_r^i \cdot F^i \qquad i = \{\mathrm{H_2O}\} \tag{10}$$

• Purity of component i in the distillate and bottoms product

$$x_{\mathrm{NT}}^i \geq \tau_c^i \qquad i = \{\mathrm{C_2H_5OH}\} \tag{11}$$

$$x_1^i \geq \tau_r^i \qquad i = \{\mathrm{H_2O}\} \tag{12}$$

• The total equilibrium stages are the active trays in the final configuration of the column

$$\mathrm{NT} = \sum_{n \in \mathrm{NTC}} \mathrm{STG}_n \tag{13}$$

• Column diameter, reboiler, and condenser areas

$$\mathrm{CD} \geq g(T_n^{\mathrm{V}}, P_n, \mathrm{VAP}_n) \qquad n \in \mathrm{NTC} \tag{14}$$

$$\mathrm{RA} \geq \frac{\mathrm{QR}}{U^{\mathrm{R}}} \cdot \left(T^{\mathrm{S}} - T_1^{\mathrm{L}}\right) \tag{15}$$

$$\mathrm{CA} \geq \frac{\mathrm{QC}}{U^{\mathrm{C}}} \cdot \left(T_{\mathrm{NT}}^{\mathrm{V}} - T^{\mathrm{CW}}\right) \tag{16}$$

where the values of U^{C} and U^{R} are 3000 and 7000 kJ/(h m^2 K), respectively. In the above equation, $T^{\mathrm{S}} = 298$ K and $T^{\mathrm{CW}} = 450$ K. Moreover, $g(T_n^V, P_n, \mathrm{VAP}_n)$ defines the equation used to compute the diameter of the column and can be consulted elsewhere.[38]

• MESH equations for the feed tray (fixed tray)

$$F_n^i + L_{n+1}^i + V_{n-1}^i - L_n^i - V_n^i = 0 \qquad n \in \mathrm{NFT} \tag{17}$$

$$F_n^i + L_{n+1}^i - L_n^i = 0 \qquad i = \{\mathrm{IL}\},\ n \in \mathrm{NFT} \tag{18}$$

$$F_n^i = \mathrm{FT} x_f^i \qquad f = \{\mathrm{ILF}, \mathrm{AMF}\},\ n \in \mathrm{NFT} \tag{19}$$

$$L_n^i = \mathrm{LIQ}_n x_n^i \qquad n \in \mathrm{NFT} \tag{20}$$

$$V_n^i = \mathrm{VAP}_n y_n^i \qquad n \in \mathrm{NFT} \tag{21}$$

$$\sum_{i \in C} \left\{F_n^i \mathrm{hF}_n^i + L_{n+1}^i \mathrm{hL}_{n+1}^i + V_{n-1}^i \mathrm{hV}_{n-1}^i - L_n^i \mathrm{hL}_n^i - V_n^i \mathrm{hV}_n^i\right\} = 0 \qquad n \in \mathrm{NFT} \tag{22}$$

$$\mathrm{hL}_n^i = f(T_n^{\mathrm{L}}) \qquad n \in \mathrm{NFT} \tag{23}$$

$$\mathrm{hV}_n^i = f(T_n^{\mathrm{V}}) \qquad n \in \mathrm{NFT} \tag{24}$$

$$\mathrm{hF}_n^i = f(T_n^{\mathrm{F}}) \qquad n \in \mathrm{NFT} \tag{25}$$

$$\sum_{i \in C} x_n^i = 1 \qquad n \in \mathrm{NFT} \tag{26}$$

$$\sum_{i \in C} y_n^i = 1 \qquad n \in \mathrm{NFT} \tag{27}$$

$$f_{i,n}^{\mathrm{L}} = f_{i,n}^{\mathrm{V}} \qquad n \in \mathrm{NFT} \tag{28}$$

$$f_{i,n}^{\mathrm{L}} = f(T_n^{\mathrm{L}}, P_n, x_n^i) \qquad n \in \mathrm{NFT} \tag{29}$$

$$f_{i,n}^{\mathrm{V}} = f(T_n^{\mathrm{V}}, P_n, y_n^i) \qquad n \in \mathrm{NFT} \tag{30}$$

$$T_n^{\mathrm{L}} = T_n^{\mathrm{V}} \qquad n \in \mathrm{NFT} \tag{31}$$

• Condenser MESH equations (fixed trays)

$$V_{n-1}^i - L_n^i - D^i = 0 \qquad n \in \mathrm{NCT} \tag{32}$$

$$D^i = \mathrm{DIS} y_n^i \qquad n \in \mathrm{NCT} \tag{33}$$

$$D_i R_{flux} = L_n^i \qquad n \in \mathrm{NCT} \tag{34}$$

$$L_n^i = \mathrm{LIQ}_n x_n^i \qquad n \in \mathrm{NCT} \tag{35}$$

$$V_n^i = \mathrm{VAP}_n y_n^i \qquad n \in \mathrm{NCT} \tag{36}$$

$$\sum_{i \in C} \left\{V_{n-1}^i \mathrm{hV}_{n-1}^i - L_n^i \mathrm{hL}_n^i - D^i \mathrm{hD}^i\right\} = \mathrm{QC} \qquad n \in \mathrm{NCT} \tag{37}$$

$$\mathrm{hL}_n^i = f(T_n^{\mathrm{L}}) \qquad n \in \mathrm{NCT} \tag{38}$$

$$\mathrm{hV}_n^i = f(T_n^{\mathrm{V}}) \qquad n \in \mathrm{NCT} \tag{39}$$

$$\mathrm{hD}^i = f(T_n^{\mathrm{L}}) \qquad n \in \mathrm{NCT} \tag{40}$$

$$\sum_{i \in C} x_n^i = 1 \qquad n \in \mathrm{NCT} \tag{41}$$

$$\sum_{i \in C} y_n^i = 1 \qquad n \in \mathrm{NCT} \tag{42}$$

$$f_{i,n}^{\mathrm{L}} = f_{i,n}^{\mathrm{V}} \qquad n \in \mathrm{NCT} \tag{43}$$

$$f_{i,n}^{\mathrm{L}} = f(T_n^{\mathrm{L}}, P_n, x_n^i) \qquad n \in \mathrm{NCT} \tag{44}$$

$$f_{i,n}^{\mathrm{V}} = f(T_n^{\mathrm{V}}, P_n, y_n^i) \qquad n \in \mathrm{NCT} \tag{45}$$

$$T_n^{\mathrm{L}} = T_n^{\mathrm{V}} \qquad n \in \mathrm{NCT} \tag{46}$$

• Reboiler MESH equations (fixed trays)

$$L_{n+1}^i - V_n^i - B^i = 0 \qquad n \in \mathrm{NRT} \tag{47}$$

dx.doi.org/10.1021/ie101801c |Ind. Eng. Chem. Res. 2011, 50, 5175–5190

$$L_{n+1}^{i} - L_{n}^{i} = 0 \qquad i = \{\mathrm{IL}\},\ n \in \mathrm{NRT} \tag{48}$$

$$B^{i} = \mathrm{BOT}x_{n}^{i} \qquad n \in \mathrm{NRT} \tag{49}$$

$$L_{n}^{i} = \mathrm{LIQ}_{n}x_{n}^{i} \qquad n \in \mathrm{NRT} \tag{50}$$

$$V_{n}^{i} = \mathrm{VAP}_{n}y_{n}^{i} \qquad n \in \mathrm{NRT} \tag{51}$$

$$\sum_{i \in C}\{L_{n+1}^{i}\mathrm{hL}_{n+1}^{i} - V_{n}^{i}\mathrm{hV}_{n}^{i} - B^{i}\mathrm{hB}^{i}\} = \mathrm{QR} \qquad n \in \mathrm{NRT} \tag{52}$$

$$\mathrm{hL}_{n}^{i} = f(T_{n}^{\mathrm{L}}) \qquad n \in \mathrm{NRT} \tag{53}$$

$$\mathrm{hV}_{n}^{i} = f(T_{n}^{\mathrm{V}}) \qquad n \in \mathrm{NRT} \tag{54}$$

$$\mathrm{hB}^{i} = f(T_{n}^{\mathrm{L}}) \qquad n \in \mathrm{NRT} \tag{55}$$

$$\sum_{i \in C} x_{n}^{i} = 1 \qquad n \in \mathrm{NRT} \tag{56}$$

$$\sum_{i \in C} y_{n}^{i} = 1 \qquad n \in \mathrm{NRT} \tag{57}$$

$$f_{i,n}^{\mathrm{L}} = f_{i,n}^{\mathrm{V}} \qquad n \in \mathrm{NRT} \tag{58}$$

$$f_{i,n}^{\mathrm{L}} = f(T_{n}^{\mathrm{L}}, P_{n}, x_{n}^{i}) \qquad n \in \mathrm{NRT} \tag{59}$$

$$f_{i,n}^{\mathrm{V}} = f(T_{n}^{\mathrm{V}}, P_{n}, y_{n}^{i}) \qquad n \in \mathrm{NRT} \tag{60}$$

$$T_{n}^{\mathrm{L}} = T_{n}^{\mathrm{V}} \qquad n \in \mathrm{NRT} \tag{61}$$

• The MESH equations for the intermediate trays in the rectifying and stripping sections

$$L_{n+1}^{i} + V_{n-1}^{i} - L_{n}^{i} - V_{n}^{i} = 0 \qquad n \in \mathrm{TM} \tag{62}$$

$$L_{n+1}^{i} - L_{n}^{i} = 0 \qquad i = \{\mathrm{IL}\}, n \in \mathrm{TM} \tag{63}$$

$$\mathrm{LIQ}_{n} = \sum_{i \in \mathrm{NC}} L_{n}^{i} \qquad n \in \mathrm{TM} \tag{64}$$

$$\mathrm{VAP}_{n} = \sum_{i \in \mathrm{NC}} V_{n}^{i} \qquad n \in \mathrm{TM} \tag{65}$$

$$\sum_{i \in C}\{L_{n+1}^{i}\mathrm{hL}_{n+1}^{i} + V_{n-1}^{i}\mathrm{hV}_{n-1}^{i} - L_{n}^{i}\mathrm{hL}_{n}^{i} - V_{n}^{i}\mathrm{hV}_{n}^{i}\} = 0 \qquad n \in \mathrm{TM} \tag{66}$$

$$\mathrm{hL}_{n}^{i} = f(T_{n}^{\mathrm{L}}) \qquad n \in \mathrm{TM} \tag{67}$$

$$\mathrm{hV}_{n}^{i} = f(T_{n}^{\mathrm{V}}) \qquad n \in \mathrm{TM} \tag{68}$$

$$\sum_{i \in C} x_{n}^{i} = 1 \qquad n \in \mathrm{TM} \tag{69}$$

$$\sum_{i \in C} y_{n}^{i} = 1 \qquad n \in \mathrm{TM} \tag{70}$$

$$f_{i,n}^{\mathrm{L}} = f_{i,n}^{\mathrm{V}} \qquad n \in \mathrm{TM} \tag{71}$$

$$f_{i,n}^{\mathrm{L}} = f(T_{n}^{\mathrm{L}}, P_{n}, x_{n}^{i}) \qquad n \in \mathrm{TM} \tag{72}$$

$$f_{i,n}^{\mathrm{V}} = f(T_{n}^{\mathrm{V}}, P_{n}, y_{n}^{i}) \qquad n \in \mathrm{TM} \tag{73}$$

$$T_{n}^{\mathrm{L}} = T_{n}^{\mathrm{V}} \qquad n \in \mathrm{TM} \tag{74}$$

• Material balances envelopes between the condenser and the tray n before the ethanol/water feed tray includes a permanent tray where the IL is fed, and between the reboiler and tray n before the ethanol/water feed tray:

$$\sum_{i \in C}\{F_{n}^{i} + V_{n-1}^{i} - D^{i} - L_{n}^{i}\} = 0 \qquad n > \mathrm{NTF\ and}\ n \in \mathrm{TM} \tag{75}$$

where

$$V_{n-1}^{3} = 0$$

and

$$\sum_{i \in C}\{L_{n+1}^{i} - B^{i} - V_{n}^{i}\} = 0 \qquad n < \mathrm{NTF\ and}\ n \in \mathrm{TM} \tag{76}$$

$$V_{n}^{3} = 0$$

• Thermodynamic behavior of system components

(1) Vapor pressure for components C_2H_5OH and H_2O[39] for each permanent tray and each active tray ($n \in$ NT, NFT, NCT, NRT):

$$\ln\left(\frac{P_{n}^{0,i}}{P_{c}^{i}}\right) = (1 - X_{n}^{i})\left(\mathrm{VP}_{A}^{i} \cdot X_{n}^{i} + \mathrm{VP}_{B}^{i} \cdot (X_{n}^{i})^{1.5} + \mathrm{VP}_{C}^{i} \cdot (X_{n}^{i})^{3} + \mathrm{VP}_{D}^{i} \cdot (X_{n}^{i})^{6}\right) \tag{77}$$

where

$$X_{n}^{i} = 1 - \frac{T_{n}^{\mathrm{L}}}{T_{\mathrm{c}}^{i}} \tag{78}$$

(2) Activity coefficients (UNIFAC):[40]

Because we assume that the IL is a new compound, for which no experimental physical properties information is available, a group contribution method is used to estimate activity coefficients values. Group contribution methods are aimed to compute some required properties starting from simple functional groups. Along these lines, the UNIFAC method is a reliable technique for activity coefficients estimation[40] and is given as follows for each permanent tray and each active tray ($n \in$ NT, NFT, NCT, NRT):

$$\ln \gamma_{n}^{i} = \ln \gamma_{n}^{\mathrm{C},i} + \ln \gamma_{n}^{\mathrm{R},i} \tag{79}$$

$$\ln \gamma_{n}^{\mathrm{C},i} = 1 - V_{n}^{\mathrm{C},i} + \ln V_{n}^{\mathrm{C},i} - 5q_{i}\left[1 - \frac{V_{n}^{\mathrm{C},i}}{F_{n}^{\mathrm{C},i}} + \ln\left(\frac{V_{n}^{\mathrm{C},i}}{F_{n}^{\mathrm{C},i}}\right)\right] \tag{80}$$

dx.doi.org/10.1021/ie101801c |Ind. Eng. Chem. Res. 2011, 50, 5175–5190

$$F_n^{C,i} = \frac{q_i}{\sum_j q_j x_n^j}; \quad V_n^{C,i} = \frac{r_i}{\sum_j r_j x_n^j} \tag{81}$$

$$r_i = \sum_k \nu_k^{(i)} R_k; \quad q_i = \sum_k \nu_k^{(i)} Q_k \tag{82}$$

$$\ln \gamma_n^{R,i} = \sum_k \nu_k^{(i)} \left(\ln \Gamma_{kn} - \ln \Gamma_{kn}^{(i)} \right) \tag{83}$$

$$\ln \Gamma_{kn} = Q_k \left[1 - \ln \left(\sum_m \theta_{mn} \psi_{mkn} \right) - \frac{\sum_m (\theta_{mn} \psi_{kmn})}{\sum_s \theta_{sn} \psi_{smn}} \right] \tag{84}$$

$$\theta_{mn} = \frac{Q_m X_{mn}}{\sum_s Q_s X_{sn}}; \quad X_{mn} = \frac{\sum_i \nu_m^{(i)} x_n^i}{\sum_i \sum_k \nu_k^{(i)} x_n^i} \tag{85}$$

$$\psi_{mn} = \exp \left[- \left(\frac{a_{sm}}{T_n^L} \right) \right] \tag{86}$$

(3) Vapor- and liquid-phase enthalpy for components C_2H_5OH and H_2O:[39]

$$\begin{aligned} hV_n^i = {} & CP_A^i \cdot (T_n^V - T_{ref}) + CP_B^i \cdot \frac{1}{2} \left((T_n^V)^2 - T_{ref}^2 \right) \\ & + CP_C^i \cdot \frac{1}{3} \left((T_n^V)^3 - T_{ref}^3 \right) + CP_D^i \cdot \frac{1}{4} \left((T_n^V)^4 - T_{ref}^4 \right) \\ & n \in NTC \end{aligned} \tag{87}$$

$$\begin{aligned} hL_n^i = {} & CP_A^i \cdot (T_n^L - T_{ref}) + CP_B^i \cdot \frac{1}{2} \left((T_n^L)^2 - T_{ref}^2 \right) \\ & + CP_C^i \cdot \frac{1}{3} \left((T_n^L)^3 - T_{ref}^3 \right) + CP_D^i \cdot \frac{1}{4} \left((T_n^L)^4 - T_{ref}^4 \right) \\ & - \lambda_i \cdot \left[\frac{1 - (T_n^L / T_c^i)}{1 - (T_{BP}^i / T_c^i)} \right]^{0.38} \qquad n \in NTC \end{aligned} \tag{88}$$

where T_{ref} = 298 K.

(4) Liquid-phase enthalpy for ionic liquids:

To develop the energy balance, it is necessary to calculate the enthalpy of the IL. This property can be estimated using the heat capacity. Ge et al.[41] predicted the heat capacity of ILs, using the principle of corresponding states, and the ideal gas heat capacity is determined using the modified Lydersen−Jobak−Reid group contribution method. The critical properties that are used in the principle of corresponding states are predicted using the group contribution method developed by Valderrama et al.[42]

The principle of corresponding states equation is given as[41]

$$\begin{aligned} \frac{C_{p,n}^L - C_{p,n}^0}{R} = {} & 1.586 + \frac{0.49}{1 - T_{r,n}} \\ & + \omega^{IL} \left[4.2775 + \frac{6.3(1 - T_{r,n})^{1/3}}{T_{r,n}} + \frac{0.4355}{1 - T_{r,n}} \right] \end{aligned} \tag{89}$$

The ideal-gas heat-capacity equation is given as[41]

$$\begin{aligned} C_{p,n}^0(T_n^L) = {} & \left[\sum_k (n_k A_{Cpk}) - 37.93 \right] \\ & + \left[\sum_k (n_k B_{Cpk}) - 0.210 \right] T_n^L \\ & + \left[\sum_k (n_k C_{Cpk}) - 3.91 \times 10^{-4} \right] (T_n^L)^2 \\ & + \left[\sum_k (n_k D_{Cpk}) - 2.06 \times 10^{-7} \right] (T_n^L)^3 \end{aligned} \tag{90}$$

The modified Lydersen−Jobak−Reid is summarized in the following equations:[42]

$$T_b^{IL} = 198.2 + \sum_k (n_k \Delta T_{bk}) \tag{91}$$

$$T_c^{IL} = \frac{T_b^{IL}}{A_M + B_M \sum_k (n_k \Delta T_{ck}) + \left[\sum_k (n_k \Delta T_{ck}) \right]^2} \tag{92}$$

$$P_c^{IL} = \frac{MW^{IL}}{\left[C_M + \sum_k (n_k \Delta P_{ck}) \right]^2} \tag{93}$$

$$\begin{aligned} \omega^{IL} = {} & \frac{(T_b^{IL} - 43)(T_c^{IL} - 43)}{(T_c^{IL} - T_b^{IL})(0.7 T_c^{IL} - 43)} \log \left(\frac{P_c^{IL}}{P_b} \right) \\ & - \left(\frac{T_c^{IL} - 43}{T_c^{IL} - T_b^{IL}} \right) \log \left(\frac{P_c^{IL}}{P_b} \right) + \log \left(\frac{P_c^{IL}}{P_b} \right) - 1 \end{aligned} \tag{94}$$

where P_b = 1.01325 bar. The enthalpy of the IL reads as follows:[39]

$$\Delta H_n^{IL} = \int_{T_{ref}}^{T_n^L} C_{p,n}^L \, dT \tag{95}$$

Merging the IL enthalpy with the ideal-gas heat capacity and the principle of corresponding states equations yields

$$\begin{aligned} hL_n^{IL} = {} & R \Big[\Big(3.15 T_c^{IL} \ln \Big\{ \left[T_c^{IL} (T_c^{IL} - T_{ref}) \right]^{1/3} \\ & + (T_c^{IL} - T_{ref})^{2/3} + (T_c^{IL})^{2/3} \Big\} \\ & - 3.5 T_c^{IL} \ln \Big\{ \left[T_c^{IL} (T_c^{IL} - T_n^L) \right]^{1/3} + (T_c^{IL} - T_n^L)^{2/3} + (T_c^{IL})^{2/3} \Big\} \\ & - 6.3 T_c^{IL} \ln \left[(T_c^{IL} - T_{ref})^{1/3} - (T_c^{IL})^{1/3} \right] \\ & + 6.3 T_c^{IL} \ln \left[(T_c^{IL} - T_n^L)^{1/3} - (T_c^{IL})^{1/3} \right] \\ & + 0.4355 T_c^{IL} \ln (T_c^{IL} - T_{ref}) - 0.4355 T_c^{IL} \ln (T_c^{IL} - T_n^L) \\ & + 10.9119 T_c^{IL} \arctan \left\{ \frac{\left[2 (T_c^{IL} - T_{ref})^{1/3} + (T_c^{IL})^{1/3} \right] \sqrt{3}}{3 (T_c^{IL})^{1/3}} \right\} \\ & - 10.9119 T_c^{IL} \arctan \left\{ \frac{\left[2 (T_c^{IL} - T_n^L)^{1/3} + (T_c^{IL})^{1/3} \right] \sqrt{3}}{3 (T_c^{IL})^{1/3}} \right\} \end{aligned}$$

dx.doi.org/10.1021/ie101801c |Ind. Eng. Chem. Res. 2011, 50, 5175–5190

$$- 18.9(T_c^{IL})^{2/3}\left(T_c^{IL} - T_{ref}\right)^{1/3} + 18.9(T_c^{IL})^{2/3}\left(T_c^{IL} - T_n^{L}\right)^{1/3}$$
$$- 4.2775T_{ref} + 4.2775T_n^{L})\omega^{IL} + 0.49T_c^{IL}\ln\left(\frac{(T_c^{IL} - T_{ref})}{(T_c^{IL} - T_n^{L})}\right)$$
$$- 1.586(T_{ref} - T_n^{L})] - a(T_{ref} - T_n^{L}) - b\left(\frac{{T_{ref}}^2 - (T_n^{L})^2}{2}\right)$$
$$- c\left(\frac{{T_{ref}}^3 - (T_n^{L})^3}{3}\right) - c\left(\frac{{T_{ref}}^4 - (T_n^{L})^4}{4}\right) - 5.15 \times 10^{-8}{T_{ref}}^4$$
$$+ 5.15 \times 10^{-8}(T_n^{L})^4 + 0.000137{T_{ref}}^3 - 0.00013(T_n^{L})^3$$
$$- 0.105{T_{ref}}^2 + 0.105(T_n^{L})^2 + 37.93T_{ref} - 37.93T_n^{L} \quad (96)$$

where

$$a = \sum_k (n_k A_{Cpk}); \quad b = \sum_k (n_k B_{Cpk});$$
$$c = \sum_k (n_k C_{Cpk}); \quad d = \sum_k (n_k D_{Cpk}) \quad (97)$$

Disjunctive Constraints. Disjunctions are constraints of the following form:

$$\vee_{j \in D}\{a_j \le g(\mathbf{w}) \le b_j\} \quad (98)$$

where a_j and b_j are, respectively, lower and upper bounds enforced on $g(\mathbf{w})$, $\mathbf{w}$ is a set of decision variables, and D is the set of disjunctions. It is well-known[43] that disjunctions can be formulated in different manners, through the introduction of binary variables $\mathbf{y}$, such as the following ones:

$$\sum_j y_j(g_j(\mathbf{w}) - b_j) \le 0 \quad (99)$$

$$\sum_j y_j(a_j - g_j(\mathbf{w})) \le 0 \quad (100)$$

$$\sum_j y_j = 1 \quad (101)$$

However, normally we do not use the above approach for handling disjunctions, because it introduces nonconvexities. Instead, the use of the big-M approach is preferred:

$$\sum_j a_j + M(1 - y_j) \le g_j(\mathbf{w}) \le b_j + M(1 - y_j) \quad (102)$$

$$\sum_j y_j = 1 \quad (103)$$

To have a clear idea about which manner of handling disjunctions is more effective, the size of the feasible region generated when the binary variables are relaxed to continuous variables is evaluated. Hence, as the size of the feasible region around the disjunctions becomes smaller, this translates into a tighter optimization formulation, improving the numerical performance when solving MINLPs. Therefore, tight disjunctive optimization formulations are highly desirable. Normally, the value of the big-M parameter is chosen on an iterative basis. The user starts with a sufficiently large M initial value that continues to decrease until no optimal solution can be determined. More details about other way of addressing disjunctions (i.e., disaggregated variables) and an example showing the impact on the size of the feasible region of the different ways of handling disjunctions can be found elsewhere.[44]

Regarding the modeling of disjunctions for the problem addressed in the present work, we remark the following points:

- These constraints are the ones associated with the discrete choice of enforcing (or not enforcing) the vapor−liquid equilibrium in a given tray. The boolean variable Z_n takes a value of "true" when the tray is selected, and, hence, the equilibrium equations are applied in that tray. In this case, the fugacities of the liquid and vapor streams are calculated, and the temperatures of liquid and vapor streams are set equal. If Z_n takes a value of "false", the composition of the inlet liquid stream is set equal to the composition of the outlet liquid stream. The vapor streams are treated similarly, and the temperatures of liquid and vapor streams entering and leaving the tray are set to those of the tray above and below, respectively. Because the equilibrium equations are not used, the values of the fugacity of the liquid and vapor phases are set to zero. The disjunction reads as follows:

$$\begin{bmatrix} Z_n \\ L_{n+1}^i + V_{n-1}^i - L_n^i - V_n^i = 0 \\ L_{n+1}^i - L_n^i = 0, i = \{\mathrm{IL}\} \\ \sum_{i \in C} x_n^i = 1 \\ \sum_{i \in C} y_n^i = 1 \\ f_{i,n}^{L} = f(T_n^{L}, P_n, x_n^i) \\ f_{i,n}^{V} = f(T_n^{V}, P_n, y_n^i) \\ f_{i,n}^{L} = f_{i,n}^{V} \\ T_n^{L} = T_n^{V} \\ L_n^i = \mathrm{LIQ}_n x_n^i \\ V_n^i = \mathrm{VAP}_n y_n^i \\ \sum_{i \in C}\{L_{n+1}^i \mathrm{hL}_{n+1}^i + V_{n-1}^i \mathrm{hV}_{n-1}^i - L_n^i \mathrm{hL}_n^i - V_n^i \mathrm{hV}_n^i\} = 0 \\ \mathrm{hL}_n^i = f(T_n^{L}) \\ \mathrm{hV}_n^i = f(T_n^{V}) \\ \mathrm{STG}_n = 1 \end{bmatrix} \vee \begin{bmatrix} \wedge Z_n \\ \\ \\ \\ \\ x_n^i = x_{n+1}^i \\ y_n^i = y_{n-1}^i \\ L_n^i = L_{n+1}^i \\ V_n^i = V_{n-1}^i \\ T_n^{L} = T_{n+1}^{L} \\ T_n^{V} = T_{n-1}^{V} \\ f_{i,n}^{L}, f_{i,n}^{V} = 0 \\ \\ \\ \mathrm{STG}_n = 0 \end{bmatrix} \quad n \in TM \quad (104)$$

As previously mentioned, the big-M formulation is applied for handling the nonlinear disjunctive programming problem, because, when the value of the M parameter is properly chosen, it yields a tight bound and does not require a disaggregation of variables.[1]

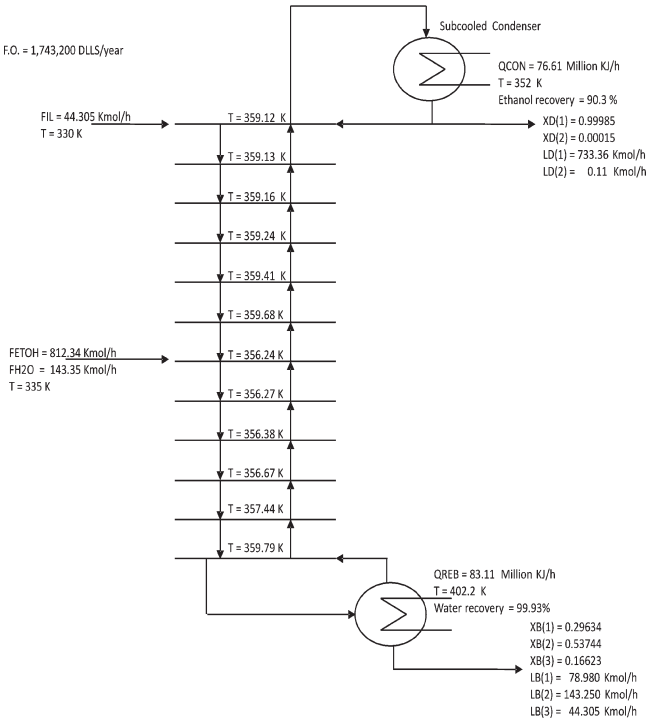

Figure 3. Results from a column with 13 equilibrium stages, where the feed tray was located in the seventh tray. Trays are numbered from bottom to top. (Legend: (1) ethanol, (2) water, and (3) IL.)

• Because there exists the possibility of deleting or deactivating different intermediate trays for the same total number of trays, it is possible to obtain multiples solutions with the same objective function value. To avoid this situation, the following set of logic constraints enforce the selected trays to be activated above and below the feed tray:

$$Z_n \Rightarrow Z_{n-1} \quad n > \mathrm{NFT} \tag{105}$$

$$Z_{n-1} \Rightarrow Z_n \quad n < \mathrm{NFT} \tag{106}$$

Strategy of Solution. The strategy to solve the MINLP model presented in this work, which optimizes the configuration of the extractive distillation to separate high-purity ethanol from the ethanol/water azeotropic mixture, using the IL 1-ethyl-3-methylimidazolium dimethylphosphate [emim][DMP] as a separation mass agent, is as follows (all the NLP problems are solved using the CONOPT solver available in GAMS, whereas Sbb is used for solving MINLP problems):

(1) Definition of the upper and lower bounds of the continuous variables of MINLP, according to the physics of the system.

(2) Simulation of the extractive distillation column shown in Figure 3. Equations 2−91 of the MINLP model equations are used in the simulation phase. The binary variables and their respective equations are not considered, because the configuration of the column is fixed.

(3) Definition of the initial values of continuous variables, obtained from the results of the simulation in step 2.

(4) Nonlinear programming (NLP) model solution (eqs 2−94). In this step, the column structure is fixed as follows: six equilibrium stages in the rectifying zone and five equilibrium stages in the stripping zone. Moreover, the four permanent equilibrium stages—condenser at saturation, IL feed stream stage, azeotropic mixture feed stage, and reboiler—are also fixed. The activity coefficients of ethanol and water are calculated using the Wilson equation. The objective function value of the model is minimized (eq 1).

(5) The results obtained in step 4 are used to estimate the initial values of the variables of the UNIFAC method and to provide good initial guesses for the values of some of the decision variables (liquid and vapor flows, compositions, temperature profile, etc). With this information, the NLP model is optimized as in step 4, but now, the activity coefficients of ethanol and water are determined by the UNIFAC method.

(6) MINLP model (eqs 1−94) solution using the results of step 5 as initial values and defining initial values for the binary variables corresponding to the conditional stages.

Solving complex MINLP problems, in general terms, is not an easy task. In fact, finding an optimal solution is strongly dependent on the initial guesses (and proper bounds) of the decision variables. We do not claim that the above proposed solution strategy is general; in fact, it completely lacks any theoretical foundation. Theoretically based optimization decomposition techniques have been proposed elsewhere.[45,46] A good initialization procedure relies on solving different versions of the same problem, starting from simple ones and progressing until the complete problem is finally approached. Of course, the idea is to use an optimal solution obtained from a given problem as an initial guess of a more-complex version of the same problem. Fortunately, from the knowledge of the problem we would like to solve, most of the time, we have a good idea about how to decompose a complex problem in simpler parts. Finally, we would like to stress that we arrived at the strategy used for solving the MINLP by trial and error. Sometimes this is the manner how complex optimization problems are solved. The difficulty for solving complex MINLPs cannot totally be appreciated by just examining the proposed solution strategy. Knowledge and intuition are valuable tools for proposing efficient decomposition and initialization strategies.

4. RESULTS AND DISCUSSION

Normally, ethanol/water mixtures are obtained from fermentation processes. After centrifugation and solids separation, the resulting ethanol/water mixture is a rather dilute mixture. In this work, we assume that a distillation column is used to raise the ethanol composition, removing most of the water and resulting in a mixture near its azeotropic composition. Because ILs generally have a tendency to be expensive compounds, it makes sense to use them only for the hard separation task region. Therefore, to address the optimal synthesis of the distillation column, we will assume that the ethanol/water main feed stream has a composition near its azeotropic composition point, obtained as mentioned previously.

Before carrying out the optimal synthesis of the extractive distillation column, a 13-equilibrium-stage column equipped with a subcooled condenser was designed and simulated to verify the modified MESH model of this work, and to obtain initial values for the synthesis process. The ethanol/water feed stream was located at the middle of the column, in stage 7, whereas the IL feed stream was located in stage 13 (see Figure 3). The product constraints to be met are as follows: (a) ethanol purity should be at least 99.5 mol % and (b) at least 90% of the ethanol present in the main feed stream should be recovered. The reflux to the

Table 1. Flows and Compositions of the 13-Equilibrium-Stage Column with the Feed Tray in the Seventh Tray

					Composition Profile[a]				
			Flow Profile		Liquid			Vapor	
feed	product	stage	LIQ	VAP	x_1	x_2	x_3	y_1	y_2
	266.6	1		1922.3	0.29634	0.53744	0.16623	0.66050	0.33950
		2	2188.8	2066.0	0.61615	0.36360	0.02024	0.84154	0.15846
		3	2332.5	2081.5	0.77924	0.20177	0.01899	0.92122	0.07878
		4	2348.0	2087.3	0.85028	0.13085	0.01887	0.95227	0.04773
		5	2353.8	2089.5	0.87799	0.10319	0.01882	0.96346	0.03654
		6	2356.0	2090.2	0.88798	0.09321	0.01881	0.96735	0.03265
955.7		7	2356.8	2033.8	0.89146	0.08974	0.01880	0.96869	0.03131
		8	1344.6	2021.6	0.91978	0.04727	0.03295	0.98617	0.01383
		9	1332.5	2023.1	0.94584	0.02091	0.03325	0.99409	0.00591
		10	1334.0	2023.9	0.95790	0.00889	0.03321	0.99752	0.00248
		11	1334.8	2024.3	0.96313	0.00368	0.03319	0.99898	0.00102
		12	1335.2	2024.5	0.96535	0.00146	0.03318	0.99960	0.00040
44.3		13	1335.3	1960.5	0.96629	0.00053	0.03318	0.99985	0.00015
Conden	733.4		1227.0		0.99985	0.00015			

[a] Subscripts legend in this table: 1, C_2H_5OH, 2, H_2O; and 3, IL.

column must be equal or greater than 10% of the distillate flow. The column configuration was similar to that which we reported in another work;[2] however, in that case, the energy balance was not taken into account. The design requirements were met using the following design values: the reflux ratio is 1.67; the thermal duties of the reboiler and condenser are 83.11 and 76.61 $\times$ 10^6 kJ/h, respectively; and the ethanol purity is 0.99985 mol fraction. Moreover, the objective function value is 1.74 $\times$ 10^6 dollars/yr. In Figure 3, the fixed configuration and main results (purity of ethanol in the top product, characteristics of the bottom product, thermal duties of the condenser, and the reboiler and temperature stage by stage) of the column are shown, whereas, in Table 1, liquid and vapor flows, as well as mole fractions in the trays of the distillation column, are presented. The results indicate that ~90% of the ethanol contained in the main feed stream can be recovered with high purity. However, because the distillation column was not optimally designed, there exists the possibility of improving this design using optimization techniques. As discussed later, this was the case for the separation task addressed in this work. The problem statistics are as follows: the number of constraints is 4441 and the number of continuous variables is 4412. CPU time is 0.391 s, using GAMS/CONOPT. All the problems were solved using a laptop computer with 4 GB RAM, 2 GHz, and an Intel Core 2 Duo processor.

For the synthesis of the extractive distillation column, the MINLP optimization formulation is applied for determining the optimal structure and operational parameters and solved using Sbb, which is a branch-and-bound algorithm available in GAMS. The structure of the column and some operational parameters of the optimization results are shown in Figure 4. The extractive distillation column obtained has 11 equilibrium stages, including the total condenser. The ethanol/water azeotropic stream was fed into stage 3, whereas the IL stream was fed in stage 10. The reboiler and condenser duties are 46.7 and 50.6 $\times$ 10^6 kJ/h, respectively. The reflux ratio is 0.57, and the objective function is 0.87 $\times$ 10^6 dollars/yr. Moreover, the amount of recovered ethanol increased slightly, up to 92%. The results clearly indicate

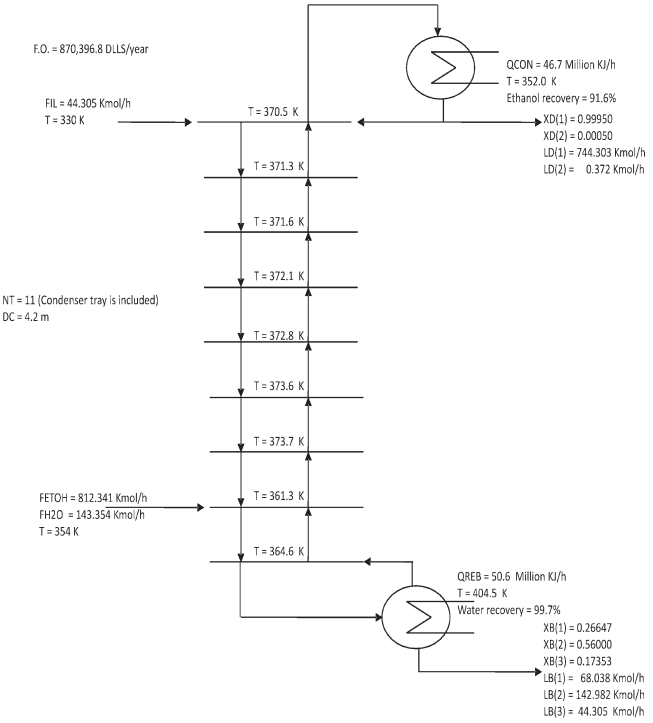

Figure 4. Results of the optimal synthesis of the distillation column. Trays are numbered from bottom to top. (Legend: (1), ethanol; (2), water; and (3), IL.)

the advantages of deploying optimization techniques for the addressed separation problem. Indeed, there is a 100% improvement in the economics profit when the separation equipment is designed by optimization strategies. Because the method used to solve the MINLP optimization problem is a local optimization algorithm, the global optimum is not guaranteed. The liquid and vapor flow rates, and the mole fraction profiles, are shown in Table 2. The problem statistics are as follows: the number of

Table 2. Flows and Composition Profiles of the Optimal Synthesized Column

			Flow Profile		Composition Profile[a]				
					Liquid			Vapor	
feed	product	stage	LIQ	VAP	x_1	x_2	x_3	y_1	y_2
	255.3	1		1160.5	0.26645	0.56000	0.17353	0.62487	0.37513
		2	1415.8	1237.9	0.56024	0.40847	0.03129	0.82916	0.17084
955.7		3	1493.2	1265.7	0.73295	0.23738	0.02967	0.91342	0.08658
		4	565.3	1237.7	0.72844	0.19319	0.07840	0.93479	0.06521
		5	537.3	1237.4	0.76803	0.14951	0.08250	0.95144	0.04856
		6	537.0	1239.0	0.80631	0.11119	0.08250	0.96528	0.03472
		7	538.6	1240.4	0.83856	0.07918	0.08226	0.97609	0.02391
		8	540.1	1242.0	0.86373	0.05424	0.08204	0.98404	0.01596
		9	541.6	1242.0	0.88230	0.03590	0.08180	0.99892	0.00108
44.3		10	541.6	1169.9	0.91640	0.00180	0.08180	0.99950	0.00050
	744.7	11	425.3		0.99950	0.00050			

[a] Subscripts legend in this table: 1, C_2H_5OH, 2, H_2O; and 3, IL.

Table 3. Big-*M* Values for Disjunctive Constraints

description	big-*M* value
liquid flows of component *i*	3000 kg mol/h
vapor flows of component *i*	3000 kg mol/h
equilibrium relationship	5 bar
vapor pressure	10 bar
composition difference between liquid streams of adjacent trays	0.3 mol fraction
composition difference between vapor streams of adjacent trays	0.3 mol fraction
flow difference between liquid streams of adjacent trays	600 kg mol/h
flow difference between vapor streams of adjacent trays	600 kg mol/h

constraints is 17 266, whereas the number of binary variables is 44 and the number of continuous variables is 15 908. CPU time is 686 s, and the absolute and relative gaps are nil, respectively; 149 nodes are visited, 151 NLPs are solved, and 6180 iterations are taken. Furthermore, in Table 3, the values of the *M* parameters for handling the disjunctive constraints are shown.

Because the interaction between the IL and the azeotropic mixture components occurs predominantly in the liquid phase, to enhance contact time, the IL is fed in the top part of the extractive column. Because the solvent (IL) is fed in the top tray, it will be present in the liquid phase of all of the stages below. The results indicate that the azeotropic mixture must be fed near the bottom of the column, because this promotes longer contact time between the azeotropic mixture and the solvent (IL), therefore achieving higher ethanol recovery in the distillate. In addition, the energy consumption was reduced when the reflux ratio was decreased, as can be seen from the 13-equilibrium-stage column results and the results obtained when the column was optimally designed. In fact, this is the main reason why the optimized process ultimately features a much better economic profit: decreasing the reflux flow rate requires reduced process thermal loads. Because energy use is one of the main costs associated with ethanol purification, reducing thermal loads leads to improved process profit.

Figures 5, 6, and 7 display the liquid-phase and vapor-phase composition profiles, the temperature profile, and the liquid and vapor molar flows in the synthesized extractive column, respectively. It was observed that the IL composition in the liquid phase significantly decreased between trays 2 and 3 around which the azeotropic mixture was fed (see Figure 5). In most of the remaining trays, the IL composition was kept approximately constant, except in tray 11, in which the IL was absent. The profile of ethanol composition in liquid phase displays a pronounced slope in the stripping zone and the profile is smoother in the rectifying zone. Between trays 3 and 4, there is a change in slope, because of the introduction of the azeotropic ethanol/water mixture. The profile of the water composition in the liquid phase decreases along the extractive column from the reboiler to the condenser until almost zero. On the other hand, the vapor-phase composition profiles for ethanol and water increases and decreases in an asymptotic form when they are observed from the reboiler to the condenser. These composition profiles show smooth behavior.

The temperature profile (see Figure 6) of the optimal configuration of the extractive column displays an increase between trays 3 and 4, because of mixed and absorption heats, which are originated by the contact between the ethanol/water azeotropic mixture fed in stage 3 and the IL descending from the stages above. Similar behavior of the temperature profile was reported in the works of Luyben[47] and Baharev et al.,[48] where the separation of the acetone/methanol system using extractive distillation with water as a separation agent is analyzed.

Figure 7 displays the liquid and vapor molar flow rates profiles in the optimal extractive column. The liquid molar flow rate profile displays two significant changes, which are due to the azeotropic mixture and the IL feed streams at trays 3 and 10, respectively. Meanwhile, the vapor molar flow rate profile remains constant along the column, except at tray 10, in which the IL is fed. We surmise that the absorption heat and associated vapor condensation heat increase the amount of liquid downflow along the column.[49] This can be observed in Figure 7, where there is a sudden increase of liquid flow rate between the fourth and third stages.

The results obtained from the simulation of the 13-tray distillation column cannot be directly compared with those obtained from the optimal synthesis of the extractive distillation

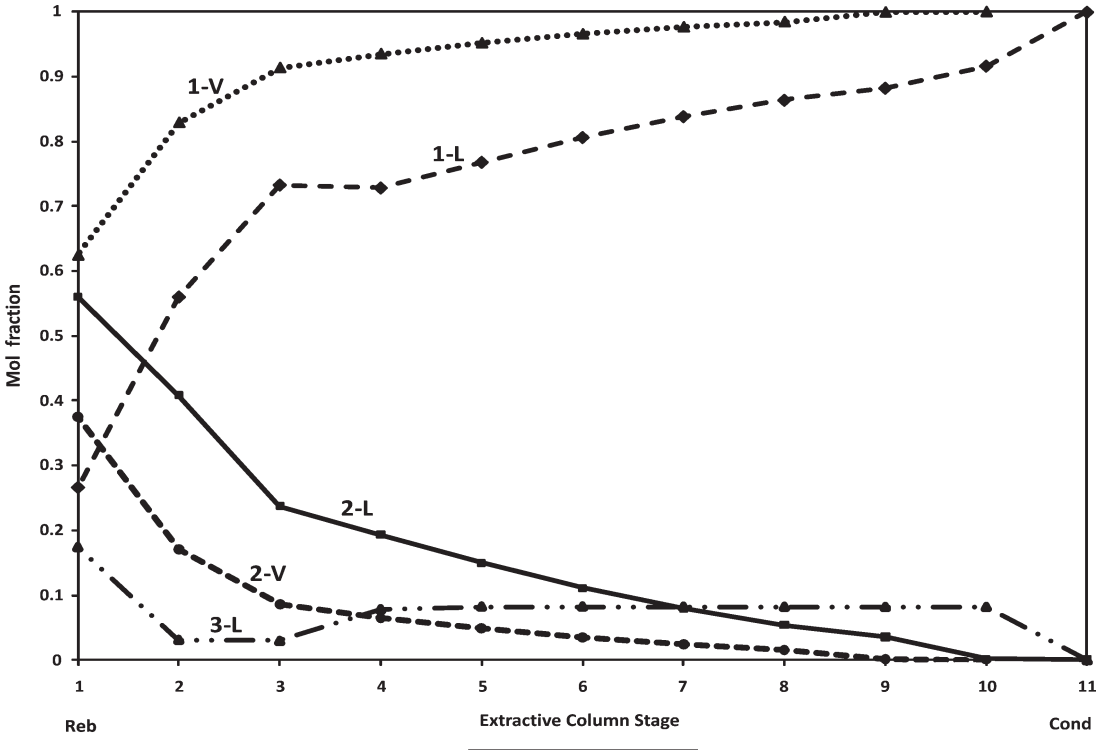

Figure 5. Liquid-phase composition profiles of ethanol (plot 1-L), water (plot 2-L), and IL (plot 3-L) and vapor-phase composition profiles of ethanol (plot 1-V) and water (plot 2-V) in the optimal extractive distillation column.

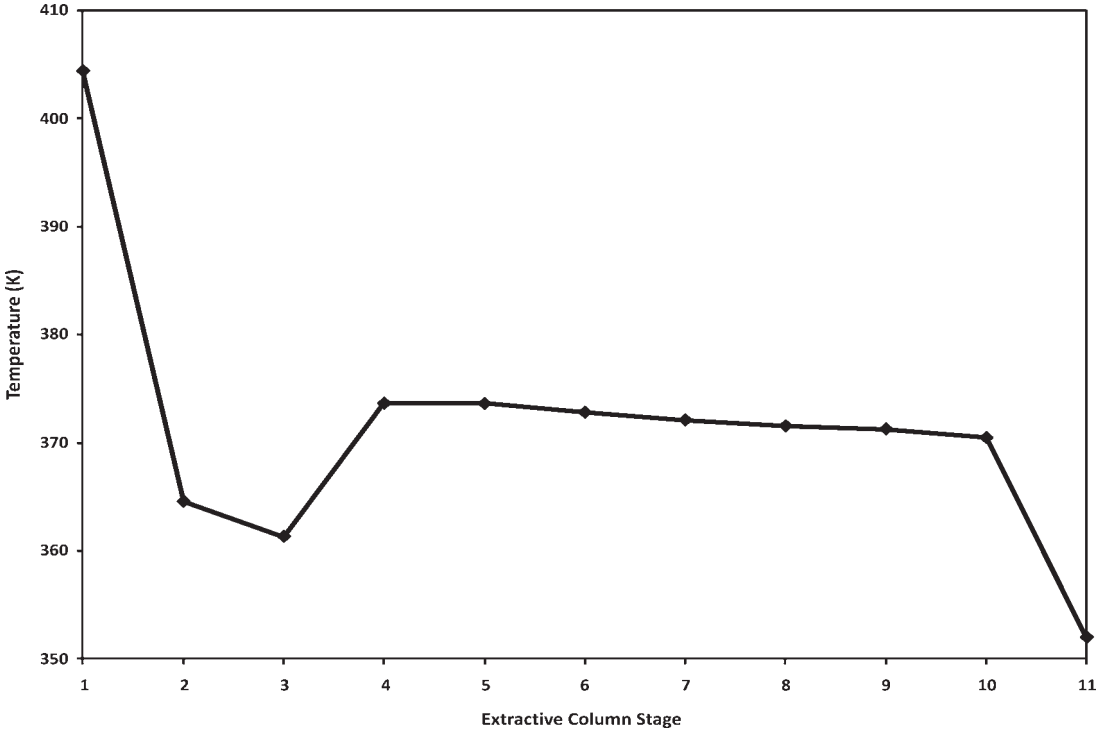

Figure 6. Temperature profile in the optimal extractive distillation column.

column, because the location of the azeotropic mixture feed stream is different. As a consequence, we decided to run a new simulation of the 13-tray column; however, in this case, the feed stream of the water/ethanol azeotropic mixture is located in the tray above the reboiler (second tray). In this way, the new configuration is more similar to that obtained from the optimization phase.

In Figure 8, the results of this new simulation are presented, whereas in Table 4, the liquid and vapor flows and the mole

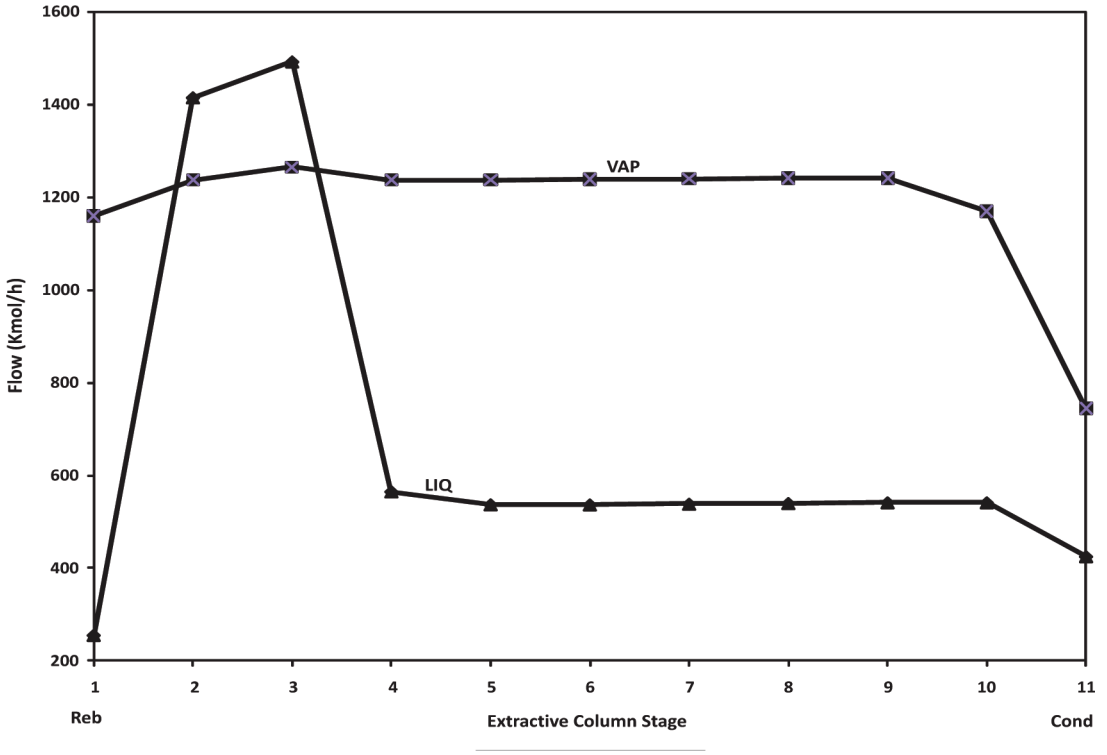

Figure 7. Liquid and vapor molar flow profiles in the optimal extractive column.

fractions in the trays of the distillation column are shown. As in the first simulation, the TAC was evaluated for comparative purposes. Comparing the results of cases with similar configurations (see Figures 4 and 8), the estimated TAC of the new simulation case is 1.3143×10^6 dollars/yr, which turns out to be 51% larger than the optimized case (see Figure 4). Similar behavior is observed in the condenser and reboiler thermal duties, which increased 37.3% and 35.5%, respectively. The ethanol recovery in the distillate product decreases by 1.42%, whereas the water recovery in the bottom product increases by 0.2%. The ethanol purity in the distillate product is slightly greater in the new simulation case, compared with the configuration of the optimized case. The behavior of water purity in the bottom product is opposite to the behavior of ethanol purity. Analyzing the above results, it can be seen that, despite the similarity between the configurations of the two cases, the extractive distillation column optimized by mathematical programming techniques has improved the design parameters, which decreases the total annual costs.

Despite the differences between the optimized and the second simulation design case, the fluctuation of the temperature profile at the bottom of the column is again observed, because of the azeotropic mixture feed stream, as can be seen from the results displayed in Figure 8. The behavior of the profiles displayed in Figures 6−8 have the same tendency, which was previously reported in two works about extractive distillation.[50,51] In the same way, the optimal synthesized separation configuration that was achieved is consistent with the results reported by Gil et al.[50] and Arifin et al.[51] Comparing the results of the simulations (see Tables 1 and 4), it can be concluded that the ethanol/water azeotropic feed tray location has a significant effect on the column behavior. When the azeotropic mixture feed stream is moved from stage 7 to stage 2, there is a significant variation in the reflux ratio (1.67 to 1.22), which, in turn, causes a reduction

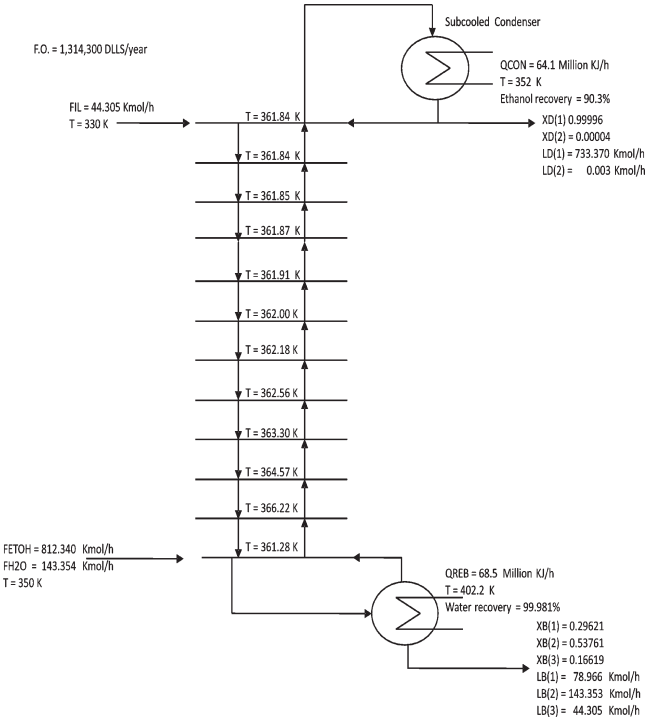

Figure 8. Results of the second column design, where the azeotropic mixture was fed in the second tray.

in the thermal duty of the reboiler (from 83.11×10^6 kJ/h to 68.5×10^6 kJ/h) and in the thermal duty of the condenser (from 76.61×10^6 kJ/h to 64.1×10^6 kJ/h). However, the ethanol purity remains constant (0.99985 versus 0.99996), to meet purity specifications. As a consequence, the objective function also

Table 4. Flows and Composition Profiles of the Column with the Feed Tray in the Second Tray

					Composition Profile[a]				
			Flow Profile		Liquid			Vapor	
feed	product	stage	LIQ	VAP	x_1	x_2	x_3	y_1	y_2
	266.6	1		1581.3	0.29621	0.53761	0.16619	0.66034	0.33966
955.7		2	1847.9	1696.1	0.60781	0.36822	0.02398	0.84435	0.15565
		3	1007.0	1683.1	0.69387	0.26214	0.04400	0.90655	0.09345
		4	994.0	1689.0	0.79721	0.15822	0.04457	0.94918	0.05082
		5	1000.0	1693.6	0.86988	0.08581	0.04431	0.97449	0.02551
		6	1004.5	1696.3	0.91291	0.04298	0.04411	0.98783	0.01217
		7	1007.2	1697.7	0.93554	0.02047	0.04399	0.99435	0.00565
		8	1008.6	1698.3	0.94659	0.00948	0.04393	0.99742	0.00258
		9	1009.2	1698.6	0.95178	0.00432	0.04390	0.99883	0.00117
		10	1009.6	1698.8	0.95418	0.00194	0.04389	0.99948	0.00052
		11	1009.7	1698.9	0.95527	0.00085	0.04388	0.99977	0.00023
		12	1009.8	1698.9	0.95576	0.00036	0.04388	0.99990	0.00010
44.3		13	1009.8	1631.1	0.95599	0.00014	0.04388	0.99996	0.00004
Conden	733.4		897.7		0.99996	0.00004			

[a] Subscripts legend in this table: 1, C_2H_5OH, 2, H_2O; and 3, IL.

changes (1.74×10^6 dollars/yr to 1.31×10^6 dollars/yr). Therefore, the economic profit clearly is improved, because of a reduction in the column energy consumption.

5. CONCLUSIONS

Because of the greenhouse effect and global climatic issues, it is expected that the use of biofuels will be increased significantly over the coming years.[5] Since some biofuels lead to the separation of alcohol/water mixtures, such a separation task can sometimes be difficult to achieve, because some of these systems can result in azeotropic behavior. In the past, azeotropic mixtures have been separated using hazardous solvents. Therefore, the present challenge consists of addressing the azeotropic separation of biofuels, keeping in mind that the new separation processes should not cause harm to the environment. This is one of the main motivations of the present work: to propose new, economically attractive, and sustainable ways to carry out the purification process of biofuels. Although biofuels can be manufactured from different biomass feedstocks, we strongly believe that, by using cellulosic residues, they will become a real sustainable and alternative energy source.

In this work, the synthesis of a high-purity extractive distillation column for bioethanol separation using ionic liquids (ILs) as a separation agent was addressed. ILs are a relatively new type of solvent, whose properties can be tuned, by proper selection of cations and anions, to feature desired target properties such as low vapor pressure, reduced toxicity, etc. The optimal synthesis of the separation task was formulated as a mixed-integer nonlinear programming (MINLP) situation, using an adaptation of a previous optimization formulation proposed by Yeomans and Grossmann,[1] which included generalized disjunctive programming for handling logic decisions in optimization problems. Because the physical properties of the IL that was used in this work have not been reported in the literature, all required properties were estimated by group contribution methods. The MINLP problem was solved using the Sbb solver embedded in GAMS. The results clearly indicate the enormous importance of using optimization tools for process design. In fact, by solving the distillation column synthesis problem using MINLP optimization tools, as much as 50% economic profit improvement was achieved, when compared to a process designed on heuristic grounds. We would like to remark that, in this work, the design of the IL allowed the intended separation task and the optimal economical synthesis of the distillation column to be carried out sequentially. However, both problems feature strong interactions that could be exploited to improve the economic profit of the process. The optimal simultaneous design of both the IL and the separation scheme are worth exploring, as a way to reduce the cost of biofuels manufacturing, so that ILs can be an attractive economic option to traditional fossil fuels.

AUTHOR INFORMATION

Corresponding Author

*Phone/fax: +52(55)59504074. E-mail: antonio.flores@uia.mx. http://200.13.98.241/~antonio.

ACKNOWLEDGMENT

The authors gratefully acknowledge the financial support for this project provided by Consejo Nacional de Cienciay Tecnologia (CONACYT), México.

DEDICATION

One of the authors (A.F.T.) wishes to dedicate this work to the memory of Prof. Oscar Sanchez Daza for his support and friendship at undergraduate studies at Universidad Autónoma de Puebla (México). We will miss his always critical points of view about Mexican society. Thanks Oscar.

NOMENCLATURE

Index

i, j = components CH_3OH, H_2O, IL (ionic liquid)

k, m, s = functional groups for UNIFAC {CH_3, CH_2, H_2O, [MIM][DMP]}

n = trays of the column, numbered from bottom to top, so that the reboiler is tray 1 and the condenser tray is number NT; n = 1, 2, ..., NT
f = type of feed; f = ionic liquid feed (ILF), azeotropic mixture feed (AMF)

Sets

C = set of components present in the feeds; $C = \{i \mid i = C_2H_5OH, H_2O, IL\}$
NTC = set of number of trays in column; NTC = $\{n \mid n =$ NFT, NCT, NRT, TM$\}$
NFT = the feed trays (two), one of which is fed with ionic liquid and the second is fed with ethanol/water mixture; NFT, $n \in$ NTC
NCT = the condenser tray of the column; NCT, $n \in$ NTC
NRT = the reboiler tray of the column; NRT, $n \in$ NTC
TM = subset of trays, which are conditional in the rectification and stripping sections of the column; TM, $n \in$ NTC
u = set of decision variables

Variables

a_{sm} = UNIFAC group interaction parameter between groups s and m (K)
A_{Cpk}, B_{Cpk}, C_{Cpk}, D^i_{Cpk} = group contribution parameters for ideal gas heat capacity of the IL
A_M, B_M, C_M = coefficients
B^i = molar flow of component i in the bottom product (kmol/h)
BOT = total molar flow of bottoms (kmol/h)
CA = condenser area (m^2)
CD = column diameter (m)
$CP_{C_2H_5OH}$ = cost of ethanol product ($\times 10^3$ dollars/kmol)
CP^i_A, CP^i_B, CP^i_C, CP^i_D = constants for ideal gas heat capacity of component i
$C^0_{p,n}$ = ideal gas heat capacity in tray n (kJ/(kmol K))
$C^L_{p,n}$ = liquid heat capacity in tray n (kJ/(kmol K))
CUC = cooling utility cost ($\times 10^3$ dollars/10^6 kJ)
$D_{C_2H_5OH}$ = ethanol product (kmol/h)
D^i = molar flow of component i in the distillate product (kmol/h)
DIS = total molar flow of distillate (kmol/h)
$f(D_{C_2H_5OH})$ = flow rate of manufactured ethanol (kmol/year)
$F^{C,i}_n$ = auxiliary property of component i (surface fraction/mol fraction) in tray n (dimensionless)
f(CA) = inversion annual cost ($\times 10^3$ dollars/year)
$f^L_{i,n}$ = fugacity of component i in the liquid phase in the tray n
F^i_n = fugacity of component i in the vapor phase in the tray molar feed flow of component i in tray n (kmol/h)
f(NT, CD) = inversion annual cost ($\times 10^3$ dollars/year)
f(QC) = heating auxiliary service cost ($\times 10^6$ kJ/year)
f(QR) = cooling auxiliary services cost ($\times 10^6$ kJ/year)
f(RA) = inversion annual cost ($\times 10^3$ dollars/year)
FT = total molar feed flow (kmol/h)
hB^i = liquid molar enthalpy of component i in the bottoms ($\times 10^6$ kJ/h)
hD^i = liquid molar enthalpy of component i in the distillate ($\times 10^6$ kJ/h)
hF^i_n = liquid molar enthalpy of component i in the feed to tray n ($\times 10^6$ kJ/h)
hL^i_n = liquid molar enthalpy of component i out of the tray n ($\times 10^6$ kJ/h)
hV^i_n = vapor molar enthalpy of component i out of the tray n ($\times 10^6$ kJ/h)
IACCA = condenser cost coefficient
IACRA = reboiler cost coefficient
ICC = column cost coefficient
LIQ_n = total molar flow of liquid out of tray n (kmol/h)
L^i_n = molar liquid flow of component i out of tray n (kmol/h)
MW^{IL} = molecular weight of ionic liquid
n_k = the number of times that a group of type k appears in the IL molecule
NT = number of real trays
P^i_c = critical pressure of component i (bar)
P^{IL}_c = critical pressure of component IL (bar)
$P^{0,i}_n$ = vapor pressure of component i in tray n (bar)
P_n = pressure in tray n (bar)
QC = heat load of condenser ($\times 10^6$ kJ/h)
q_i = parameter relative to molecular van der Waals surface areas of pure component i (UNIFAC)
Q_k, Q_m, Q_s = group surface area parameter in the UNIFAC model
QR = heat load of reboiler ($\times 10^6$ kJ/h)
R = the universal gas constant(kJ/(kmol K))
RA = reboiler area (m^2)
R_{flux} = reflux ratio (dimensionless)
r_i = parameter relative to molecular van der Waals volumes of pure component i (UNIFAC)
R_k = group volume parameter in the UNIFAC model
STG_n = counter for the existence of a tray
SUC = steam utility cost ($\times 10^3$ dollars/10^6 kJ)
TAC = economic function ($\times 10^3$ dollars/year)
T^{IL}_b = normal boiling temperature of IL (K)
T^i_{BP} = normal boiling temperature of component i (K)
T^i_c = critical temperature of component i (K)
T^{IL}_c = critical temperature of IL (K)
T^{CW} = temperature of heating utility (K)
$T_{r,n}$ = reduced temperature in tray n; $T_{r,n} = T^L_n/T_c$
T_{ref} = reference temperature (K)
T^f_n = feed stream temperature to tray n (K)
T^L_n = temperature of liquid out of tray n (K)
T^V_n = temperature of vapor out of tray n (K)
T^S = temperature of cooling utility (K)
U^C, U^R = overall heat-transfer coefficient for condenser (C) and reboiler (R) (kJ/(h m^2 K))
VAP_n = total molar flow of vapor out of tray n (kmol/h)
$V^{C,i}_n$ = auxiliary property of component i (volume fraction/mol fraction) in tray n (dimensionless)
V^i_n = molar vapor flow of component i out of tray n (kmol/h)
VP^i_A, VP^i_B, VP^i_C, VP^i_D = constants for vapor pressure equation of component i
x^i_f = liquid mole fraction of component i in type of feed f
X_{mn} = fraction of group m in the mixture of liquid phase in tray n (dimensionless)
X_{sn} = fraction of group s in the mixture of liquid phase in tray n (dimensionless)
x^i_n = liquid mole fraction of component i out of tray n
x^j_n = liquid mole fraction of component j out of tray n
y^i_n = vapor mole fraction of component i out of tray n
Z_n = logic variable, the value of which can be true or false

Greek Variables

γ^i_n = activity coefficient of the component i in tray n (dimensionless) (UNIFAC)
$\gamma^{C,i}_n$ = combinatorial contribution to the activity coefficient of component i in tray n, dimensionless (UNIFAC)
$\gamma^{R,i}_n$ = residual contribution to the activity coefficient of component i in tray n, dimensionless (UNIFAC)

ξ_c^i = recovery of component i, it represents the minimum recovery fraction of component i in the distillate (mol)
ξ_r^i = recovery of component i, it represents the minimum recovery fraction of component i in the bottoms (mol)
Γ_{kn} = residual activity coefficient of group k in tray n (dimensionless) (UNIFAC)
$\Gamma_{kn}^{(i)}$ = residual activity coefficient of group k in a reference solution containing only molecules of type i in tray n (dimensionless) (UNIFAC)
ΔH_n^{IL} = change of the IL's enthalpy, with respect to one reference temperature
ΔP_{ck} = group contribution parameter for group type k, relative to the critical pressure
ΔT_{bk} = group contribution parameter for group type k, relative to the normal boiling temperature
ΔT_{ck} = group contribution parameter for group type k, relative to the critical temperature
θ_{mn} = the group fraction of group m in the mixture of liquid phase in tray n (dimensionless) (UNIFAC)
θ_{sn} = the group fraction of group s in the mixture of liquid phase in tray n (dimensionless) (UNIFAC)
λ_i = heat vaporization of component i (kJ/kmol)
$\nu_k^{(i)}$ = number of groups of type k in molecule i (UNIFAC)
$\nu_m^{(i)}$ = number of groups of type m in molecule i (UNIFAC)
τ_c^i = purity of component i; it represents the minimum purity of component i in the distillate (mole fraction)
τ_r^i = purity of component i; it represents the minimum purity of component i in the bottoms (mole fraction)
ψ_{smn}, ψ_{mkn}, ψ_{kmn} = group interaction parameters in tray n (dimensionless) (UNIFAC)
ω^{IL} = acentric factor of IL (dimensionless)

REFERENCES

(1) Yeomans, H.; Grossmann, I. E. *Ind. Eng. Chem. Res.* **2000**, *39*, 1637–1648.
(2) Chávez-Islas, L. M.; Vásquez-Medrano, R.; Flores-Tlacuahuac, A. Submitted to *Ind. Eng. Chem. Res.*
(3) Eggemand, T.; Atiyeh, C. *Chem. Eng. Prog.* **2010**, *106*, 36–38.
(4) U.S. Dept. of Energy and U.S. Dept. of Agriculture, http://feedstockreview.ornl.gov/pdf/billiontonvision.pfd , 2005.
(5) Regalbuto, J. *Comput. Chem. Eng.* **2010**, *34*, 1393−1396 (doi:10.1016/j.compchemeng.2010.02.025).
(6) Brennecke, J. F.; Maginn, E. J. *AIChE J.* **2001**, *47*, 2384–2389.
(7) Earle, M. J.; Seddon, K. R. *Pure Appl. Chem.* **2000**, *72*, 1391–1398.
(8) Qureshi, N.; Hughes, S.; Maddox, I. S.; Cotta, M. A. *Bioprocess Biosyst. Eng.* **2005**, *27*, 215–222.
(9) Morris, D.; Ahmed, I. http://www.p2pays.org/ref/24/23824.pdf , 1992.
(10) Vane, L. M. *J. Chem. Technol. Biotechnol.* **2005**, *80*, 603–629.
(11) Koczka, K.; Mizsey, K.; Fonyo, Z. *Cent. Eur. J. Chem.* **2007**, *5*, 1124–1147.
(12) Luyben, W. L. *Ind. Eng. Chem. Res.* **2009**, *48*, 3484–3495.
(13) Arifeen, N.; Wang, R.; Kookos, I. K.; Webb, C.; Koutinas, A. A. *Biotechnol. Prog.* **2007**, *48*, 1349–1403.
(14) Melsert, R. M. M.Sc. Thesis , Georgia Institute of Technology, Atlanta, GA, 2007.
(15) Vane, L. M. *Biofuels, Bioprod. Biorefin.* **2008**, *2*, 553–588.
(16) Ling, H.; Luyben, W. L. *Ind. Eng. Chem. Res.* **2009**, *48*, 6034–6049.
(17) Karuppiah, R.; Peschel, A.; Grossmann, I. E.; Martin, N.; Martison, W.; Zullo, L. *AIChE J.* **2008**, *54*, 1499–1525.
(18) Treybal, R. *Mass Transfer Operations*; McGraw−Hill Book Company: New York, 1980.
(19) Brennecke, J. F.; Maginn, E. J. *AIChE J.* **2001**, *47*, 2384–2389.
(20) Fadeev, A. G.; Meagher, M. M. *Chem. Commun.* **2001**, *3*, 295–296.
(21) Seiler, M.; Jork, C.; Kavarnou, A.; Arlt, W.; Hirsch, R. *AIChE J.* **2004**, *50*, 2439–2454.
(22) Alvarado-Morales, M.; Terra, J.; Gernaey, K. V.; Woodley, J. M.; Gani, R. *Chem. Eng. Res. Des.* **2009**, *87*, 1171–1183.
(23) Simoni, L. D.; Chapeaux, A.; Brennecke, J. F.; Stadtherr, M. A. *Comput. Chem. Eng.* **2010**, *34*, 1406−1412 (doi:10.1016/j.compchemeng.2010.02.020).
(24) Marsh, K. N.; Boxall, J. A.; Lichtenthaler, R. *Fluid Phase Equilib.* **2004**, *219*, 93–98.
(25) BASF, the Chemical Company (http://www.basionics.com/en/ionic-liquids/processes/distillation.htm).
(26) McLeese, S. E.; Eslick, J. C.; Hoffmann, N. J.; Scurto, A. M.; Camarda, K. V. *Comput. Chem. Eng.* **2010**, *34*, 1476–1480.
(27) Viswanathan, J.; Grossmann, I. E. *Ind. Eng. Chem. Res.* **1993**, *32*, 2942–2949.
(28) Turkay, M.; Grossmann, I. E. *Comput. Chem. Eng.* **1996**, *20*, 959–978.
(29) Grossmann, I. E.; Caballero, J. A.; Yeomans, H. *Lat. Am. Appl. Res.* **2000**, *30*, 263–284.
(30) Turkay, M.; Grossmann, I. E. *Ind. Eng. Chem. Res.* **1996**, *35*, 2611–2623.
(31) Yeomans, H.; Grossmann, I. E. *Comput. Chem. Eng.* **1999**, *23*, 1135–1151.
(32) Yeomans, H.; Grossmann, I. E. *Ind. Eng. Chem. Res.* **2000**, *39*, 4326–4335.
(33) Ferris, M. C.; Pandz, J. S. *SIAM Rev.* **1997**, *39*, 669–713.
(34) Ye, J. J. *SIAM J. Optim.* **1999**, *9*, 374–387.
(35) Jain, V.; Grossmann, I. E. *Informs J. Comput.* **2001**, *13*, 258–276.
(36) Outrata, J.; Kocvara, M.; Zowe, J. *Nonsmooth Approach to Optimization Problems with Equilibrium Constraints*; Kluwer Academic Publishers: Dordrecht, The Netherlands, 1998.
(37) Turkay, M.; Grossmann, I. E. *Comput. Chem. Eng.* **1996**, *20*, 959–978.
(38) Wankat, P. *Separation Process Engineering*; Prentice−Hall: Upper Saddle River, NJ, 2007.
(39) Reid, R.; Prausnitz, J.; Poling, B. *The Properties of Gases and Liquids*; McGraw−Hill: New York, 1987.
(40) Lei, Z.; Zhang, J.; Li, Q.; Chen, B. *Ind. Eng. Chem. Res.* **2009**, *48*, 2697–2704.
(41) Ge, Y.; Zhang, L.; Yuan, X.; Geng, W.; Ji, J. *J. Chem. Thermodyn.* **2008**, *40*, 1248–1252.
(42) Valderrama, J. O.; Rojas, R. E. *Ind. Eng. Chem. Res.* **2009**, *48*, 6890–6900.
(43) Grossmann, I. *Optim. Eng.* **2002**, *3*, 227–252.
(44) Flores-Tlacuahuac, A.; Biegler, L. T. *Comput. Chem. Eng.* **2008**, *32*, 2823–2837.
(45) Fisher, M. *Interfaces* **1985**, *15* (2), 10.
(46) Guignard, M. *Eur. J. Oper. Res.* **1995**, *35*, 193–200.
(47) Luyben, W. L. *Ind. Eng. Chem. Res.* **2008**, *47*, 4425–4439.
(48) Baharev, A.; Achterberg, T.; Rév, E. *AIChE J.* **2009**, *55*, 1695–1704.
(49) Van Winkle, M. *Distillation*; McGraw−Hill Book Company: New York, 1967.
(50) Gil, I. D.; Botía, D. C.; Ortiz, P.; Sánchez, O. F. *Ind. Eng. Chem. Res.* **2009**, *48*, 4858–4853.
(51) Arifin, S.; Chien, I. L. *Ind. Eng. Chem. Res.* **2008**, *47*, 790–803.